BE PART OF MAKING A SHIFT IN TYPE 2 DIABETES

With an early shift in treatment you could help reduce the risk factors associated with type 2 diabetes and help your patients avoid long-term complications.[1–3]

Shift the trajectory of type 2 diabetes

Early and intensive HbA_{1c} control, weight loss and reduction of risk factors are essential to prevent long-term complications associated with type 2 diabetes.[4–6]

With uncontrolled HbA_{1c} a 1% drop could make all the difference.

The closer people living with type 2 diabetes are to their target HbA_{1c}, the lower the risk of complications in the future. Observational and clinical trial analyses suggest that a 1% reduction in HbA_{1c} has the potential to reduce the risk of complications and prevent deaths related to diabetes.[4,7]

You play an important role in type 2 diabetes management by making sure your patients are getting the treatment that is right for them and the advice they need to stay on track.

---

*To learn how an early **shift** in treatment could lead to better health outcomes for your patients,* ***visit Novo Nordisk***

LEARN MORE

References

1. Correa MF, Li Y, Kum H-C et al. Assessing the Effect of Clinical Inertia on Diabetes Outcomes: a Modeling Approach. J Gen Intern Med 2019;34:372–378. **2.** Paul SK, Klein K, Thorsted BL et al. Delay in treatment intensification increases the risks of cardiovascular events in patients with type 2 diabetes. Cardiovasc Diabetol. 2015;14:100.**3.** Khunti K, Wolden ML, Thorsted BL et al. Clinical inertia in people with type 2 diabetes: a retrospective cohort study of more than 80,000 people. Diabetes Care. 2013;36:3411–3417 **4.** Lind M, Imberg H, Coleman RL et al. Historical HbA1c, values may explain the type 2 diabetes legacy effect: UKPDS 88. Diabetes Care.2021;44(10):2231-2237. **5.** Burke GL, Bertoni AG, Shea S, et al. The impact of obesity on cardiovascular disease risk factors and subclinical vascular disease. Archives of Internal Medicine. 2008;168(9):928. **6.** Mendis S, Puska P, Norrving B. Global Atlas on Cardiovascular Disease Prevention and Control. World Health Organization, Geneva 2011. **7.** Stratton IM, Adler AI, Neil HA et al. Association of glycaemia with macrovascular and microvascular complications of type 2 diabetes (UKPDS 35): Prospective Observational Study. BMI. 2000;321(7258):405-412.

June 2023 | HQ23DI00055

novo nordisk®

ESC HEART FAILURE
ESC Heart Failure (2023)
Published online in Wiley Online Library (wileyonlinelibrary.com) **DOI:** 10.1002/ehf2.14522

ORIGINAL ARTICLE

Phenotyping congestion in acute heart failure by renal flow and right heart to pulmonary circulation coupling

Alessandro Vella[1], Valentina Labate[1], Gianmarco Carenini[2], Eleonora Alfonzetti[1], Valentina Milani[1], Francesco Bandera[1], Omar Oliva[1] and Marco Guazzi[3,4]*

[1]*Policlinico San Donato, Milan, Italy;* [2]*Cardiology Division, San Gerardo Hospital, Monza, Italy;* [3]*Department of Biological Sciences, University of Milan School of Medicine, Milan, Italy; and* [4]*Cardiology Division, San Paolo Hospital, Milan, Italy*

Abstract

Aims In acute heart failure (AHF), kidney congestion is basic to treatment and prognosis. Its aetiology is manifold and quite unexplored in details mainly regarding the right heart to pulmonary circulation (Pc) coupling. We investigated the right heart to kidney interrelationship by Doppler renal flow pattern, right atrial dynamics, and right ventricular (RV) function to Pc coupling in AHF.

Methods and results In 119 AHF patients, echocardiographic and renal Doppler data were analysed. Univariate and multivariate regression models were performed to define the determinants of a quantitative parameter of renal congestion, the renal venous stasis index (RVSI). When grouped according to different intra-renal venous flow patterns, no differences were observed in haemodynamics and baseline renal function. Nonetheless, patients with renal Doppler evidence of congestion showed a reduced RV function [tricuspid annular plane systolic excursion (TAPSE), S'-wave velocity, and fractional area change], impaired RV to Pc coupling [TAPSE/pulmonary artery systolic pressure (PASP) ratio], and right atrial peak longitudinal strain (RAPLS), along with signs of volume overload [increased inferior vena cava (IVC) diameters and estimated right atrial pressure]. Univariate and multivariate regression analyses confirmed TAPSE/PASP, RAPLS, and IVC diameter as independent determinants of the RVSI. RVSI was the only variable predicting the composite outcome (cardiac death, heart failure hospitalization, and haemodialysis). An easy-to-use echo-derived right heart score of four variables provided good accuracy in identifying kidney congestion.

Conclusions In AHF, the renal venous flow pattern combined with a right heart study phenotypes congestion and clinical evolution. Keys to renal flow disruption are an impaired right atrial dynamics and RV–Pc uncoupling. Integration of four right heart echocardiographic variables may be an effective tool for scoring the renal congestive phenotype in AHF.

Keywords Congestion; Acute heart failure; Right heart; Renal Doppler

Received: 24 March 2023; Revised: 3 August 2023; Accepted: 22 August 2023
**Correspondence to: Marco Guazzi, Cardiology Division, San Paolo Hospital, Via Antonio di Rudinì, 8, 20142 Milan, Italy. Tel: +39 02 81844846. Email: marco.guazzi@unimi.it*

Introduction

In heart failure (HF), a large amount of interest has long been placed on the heart–kidney interaction in view of its strong pathophysiological and clinical relevance,[1] and this is true especially for acutely decompensated HF in which kidney and susceptibility to fluid overload and retention are central to the treatment.

There is a new-found focus on renal venous congestion and its link with right HF.[2] Despite the impressive amount of information on this topic, the complex pathophysiology of the congested kidney and its clinical significance are matters of continuous evolution. A reference non-invasive, easy-to-use, and daily practice feasible method to evaluate HF-induced renal congestion has not been found yet, but some promising perspectives come from the Doppler renal

flow quantification and an analysis of the arterial and venous patterns of organ flow dynamics.

The Doppler evaluation of intra-renal venous flow (IRVF) has been applied in the evaluation of renal haemodynamics in pregnancy, diabetes, and obstructive kidney disease[3] and, most recently, in HF,[4,5] pulmonary hypertension (PH),[6] and post-cardiac surgical setting.[7]

The information available in the HF scenario primarily concerns the chronic and stable clinical condition, and just two papers on acute HF (AHF) patients have been published.[8,9]

We therefore aimed at implementing this area of evidence linking the Doppler renal flow with right atrial (RA) dynamics and right ventricular (RV) to pulmonary circulation (Pc) coupling in AHF. In this context, we also aimed at developing a simple ultrasound-derived score, based on readily available cardiac parameters, to better phenotype and predict the extent of renal congestion in this population.

Materials and methods

Study design and population

One hundred nineteen AHF patients admitted to the HF unit of a tertiary centre community hospital were enrolled from October 2017 to December 2019. Renal Doppler data were acquired by a single operator; as such, only patients being admitted during those physician working days have been included. AHF was diagnosed based on the current guidelines criteria,[10] and all patients required intravenous (i.v.) diuretic therapy at presentation. Pregnant women and patients with end-stage chronic kidney disease (CKD Stage 5 or haemodialysis) or known obstructive kidney disease were excluded. Due to inadequate renal Doppler image quality, nine patients have been omitted from the final analysis (*Figure 1*). Clinical, ultrasound, and laboratory data were obtained on the same day of admission. Echocardiographic and renal Doppler data were acquired consecutively by the same examiner at the time of admission in our unit. Although patients received i.v. diuretics in the Emergency Department, they were all deemed still clinically decompensated at the time of enrolment and data collection. The investigation conformed to the principles outlined in the Declaration of Helsinki.

Cardiac echocardiographic evaluation

Comprehensive transthoracic echocardiography was performed according to the current guidelines.[11] RV function was assessed by tricuspid annular plane systolic excursion (TAPSE), systolic free wall myocardial velocity (S'-wave velocity), fractional area change (FAC), and TAPSE/pulmonary artery systolic pressure (PASP) ratio, a recognized non-invasive marker of RV to Pc coupling, highly prognostic in HF and PH.[12,13] RA pressure (RAP) was estimated from inferior vena cava (IVC) diameters and collapsibility[11] using a three-grade classification (5, 10, and 15 mmHg). RA size and function were assessed from standard two-dimensional (2D) and 2D speckle tracking echocardiography (STE) apical four-chamber images and cine loops, respectively, as

Figure 1 Study flow chart. AHF, acute heart failure; CKD, chronic kidney disease.

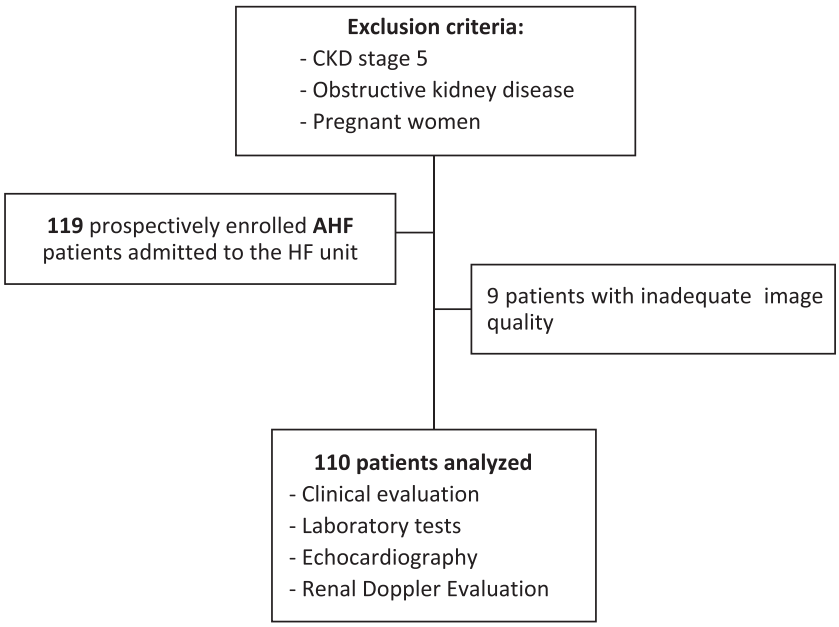

recommended.[14] RA volume index (RAVi) was estimated from RA end-systolic area. Strain analysis is detailed in the Supporting Information.

The analysis has been focused on RA peak longitudinal strain (RAPLS) as the most commonly altered atrial function parameter in both left heart dysfunction and right heart dysfunction and with high prognostic value for all-cause mortality and HF-related hospitalizations.[15]

Tricuspid regurgitation (TR) severity was evaluated using a four-grade classification (mild, moderate, severe, and massive/torrential), according to the current criteria.[16] Stroke volume (SV) and cardiac output (CO) calculations are reported in the Supporting Information.

Renal Doppler evaluation

IRVF colour and spectral Doppler evaluation were assessed with the same cardiac probe with a sector transducer frequency range of 1–5 MHz while the patient was lying in the left lateral decubitus. The colour Doppler velocity range was set to ~16 cm/s. After proper alignment, the right kidney interlobar vessels were identified recording pulsed Doppler flows. In accordance with previous reports, IRVF was evaluated in the right kidney only, due to left kidney venous flow phasicity attenuation by perpendicular renal vein confluence with the IVC and possible entrapment between the abdominal aorta and the superior mesenteric artery.[5,17] IRVFs were obtained by the mean of three measurements in sinus rhythm or three index beats (beat following two preceding cardiac cycles of equal duration) in atrial fibrillation (AF).[4] The renal resistive index (RRI)[18] was calculated as the maximum arterial flow velocity minus the diastolic flow velocity, divided by the maximum flow velocity. The venous flow pattern was categorized as continuous or discontinuous based on its morphology. Continuous pattern was defined as venous flow nadir >0 throughout the cardiac cycle. Discontinuous flows, in which the nadir reached zero, were further subdivided into pulsatile, biphasic, and monophasic, based on whether flow interruption was present just during end-diastole, end-diastole and late-systole, or when extended through most of the cardiac cycle, permitting only an early diastolic flow, respectively (*Figure 2A–D*). The venous impedance index (VII) was measured as the peak maximum flow velocity minus minimal flow velocity, divided by maximum flow velocity; therefore, VII was calculated as 1 in discontinuous patterns (*Figure 2E*). To quantitatively assess discontinuous patterns, the recently proposed index of renal congestion was calculated, that is, the renal venous stasis index (RVSI)[6] reflecting the ratio between the renal venous no-flow time and cardiac cycle duration (*Figure 2F*).

Laboratory data are reported in the Supporting Information.

Statistical analysis

Continuous variables are expressed as mean ± standard deviation (SD), when normally distributed, otherwise as median and inter-quartile range (IQR). Categorical data were expressed as frequency and percentage. Data normality was assessed by the Shapiro–Wilk test. Comparisons between two groups were performed by Student's *t*-test or Mann–Whitney *U* test for continuous variables and χ^2 test for categorical variables. One-way analysis of variance (ANOVA) was used to compare multiple variables with IRVF patterns. To assess differences between non-normally distributed variables among IRVF groups, the Kruskal–Wallis *H* test was used. A *P* value <0.05 was considered statistically significant. Spearman and Pearson correlation analysis was performed between various continuous variables and IRVF patterns, with a >0.3 relevance cut-off for coefficient values. To expose the independent determinants of RVSI, a multivariate logistic regression analysis model was built using significant univariate factors. Intra- and inter-observer reliability of IRVF pattern and RVSI assessment was determined by calculation of the weighted Cohen's kappa coefficient and intra-class correlation coefficient (ICC), respectively, on a random sample of 20 patients. A receiver operating characteristic (ROC) curve was elaborated to evaluate the performance of an echocardiographic score in predicting marked renal venous congestion (i.e. monophasic IRVF pattern or RVSI ≥ 0.75). Univariate and multivariate Cox regression analysis was performed to identify the predictors of events, assessed as composite endpoint (cardiac death, HF hospitalization, and haemodialysis initiation). All calculations were performed with SPSS Version 23.0 software (IBM Corp.).

Results

Demographic, clinical characteristics, echocardiographic, and laboratory data

Of the 119 patients, 9 had an inadequate renal venous flow image quality. As reported in Table 1, the mean age was 73 ± 12 years, with 63% males presenting in New York Heart Association (NYHA) Class III or IV (64%). The most prevalent aetiology of HF was ischaemic, followed by valvular and 'idiopathic' forms.

Systemic arterial hypertension, dyslipidaemia, smoking habit, and diabetes mellitus were highly prevalent (77%, 58%, 42%, and 39%, respectively), and the same was true for AF (previous history 48% and present during the echo examination 41%). Chronic obstructive pulmonary disease (COPD) rate was 24%. At hospital admission, diuretics, beta-blockers, and angiotensin-converting enzyme (ACE) inhibitors/angiotensin receptor blockers were part of the home

Figure 2 Venous flow patterns: (A) continuous, (B) discontinuous pulsatile, (C) discontinuous biphasic, (D) discontinuous monophasic, (E) venous impedance index, and (F) renal venous stasis index (RVSI). RVSI represents the percentage of cardiac cycle free of renal venous outflow resulting in 0 in the continuous pattern.

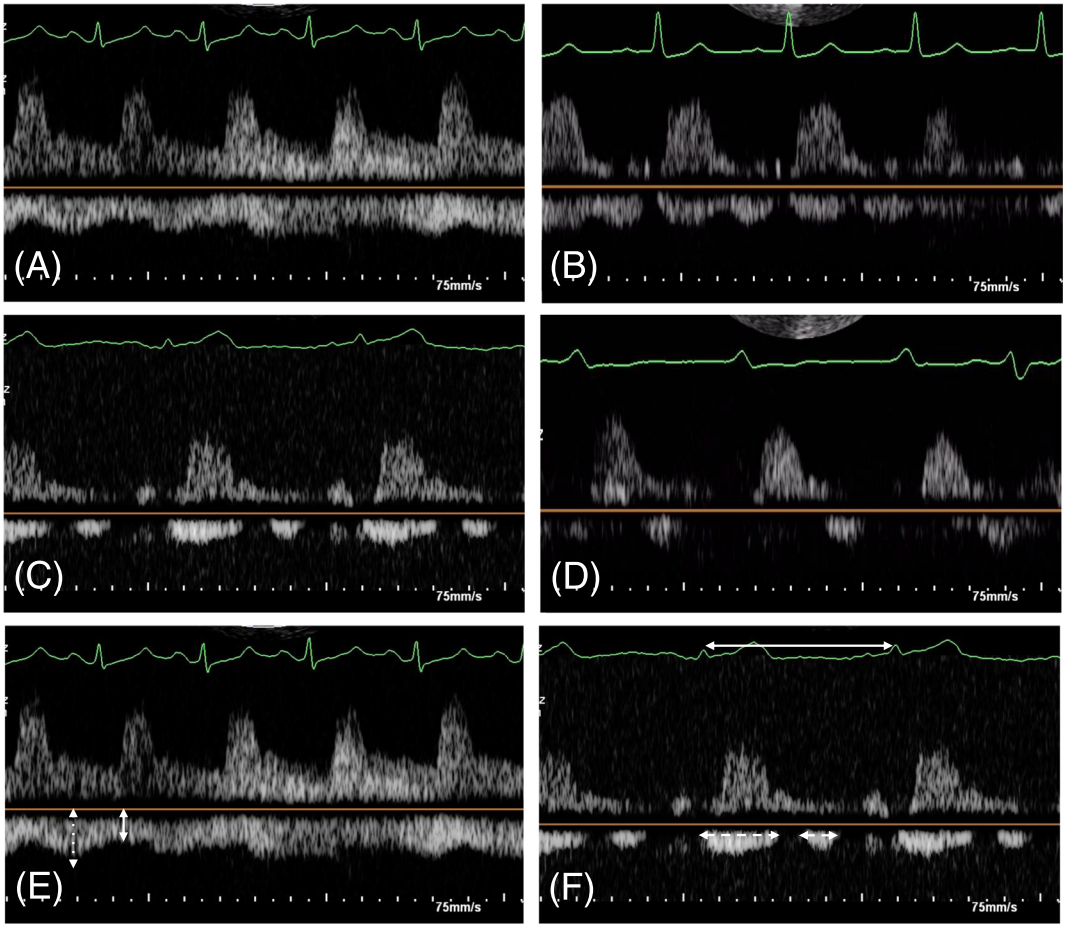

therapy in 75%, 70%, and 51% of cases. Angiotensin receptor neprilysin inhibitors (ARNIs) were taken by only 10% of patients.

The average ejection fraction (EF) was moderately reduced (41%), with HF with reduced ejection fraction (HFrEF), HF with preserved ejection fraction (HFpEF), and HF with mildly reduced ejection fraction (HFmrEF) accounting for 49%, 34%, and 17%. SV, CO, and cardiac index (CI) were slightly reduced.

RV dysfunction was highly prevalent, as shown by the average TAPSE (16 mm), S'-wave velocity (9 cm/s), FAC (36%), and TAPSE/PASP ratio (0.44).

There was evidence of biatrial enlargement, with clear depression of RA function, as expressed by a mean RAPLS of 21%.[19]

Systemic congestion was common, as suggested by increased IVC diameter with limited collapsibility and an estimated RAP (eRAP) >10 mmHg. Average left ventricular (LV) filling pressure was abnormally elevated (mean E/e' of 16).

The median creatinine was slightly elevated, with an estimated glomerular filtration rate (eGFR) of 56 mL/min. Average N-terminal pro-brain natriuretic peptide (NT-proBNP) values were markedly abnormal (3229 ng/L).

Renal haemodynamic data

The percentage of non-interpretable studies was low (7.6%), even if slightly higher compared with previous reports (3%). This small difference may be expected considering that no dedicated curvilinear probe was available in our unit at the time of the study. Kidney arterial haemodynamics were unremarkable, with a mean RRI of 0.68 and only 25% of patients showing a continuous IRVF pattern. A pulsatile, biphasic, and monophasic pattern was observed in 21%, 14%, and 33% of cases, respectively. Median RVSI was 0.56 in patients with a discontinuous renal venous flow, and median VII was 0.15 among continuous-flow phenotypes.

Table 1 Demographic, clinical characteristics, echocardiographic, and laboratory data

	All (119)	Continuous (29)	Pulsatile (25)	Biphasic (17)	Monophasic (39)	*P* value
Demographics						
Age (years)	73 ± 12	72 ± 13	77 ± 7	70 ± 11	73 ± 12	0.2814
Males, *n* (%)	69 (63)	14 (45)	13 (59)	13 (76)	29 (73)	0.0651
BSA (m^2)	1.81 ± 0.21	1.77 ± 0.18	1.82 ± 0.20	1.85 ± 0.28	1.8 ± 0.17	0.6441
Clinical data						
NYHA class, *n* (%)						0.0628
I	8 (8)	6 (21)	0 (0)	1 (6)	1 (3)	
II	30 (28)	10 (34)	6 (27)	1 (6)	13 (34)	
III	59 (56)	12 (41)	15 (68)	13 (76)	19 (50)	
IV	8 (8)	1 (3)	1 (5)	2 (12)	4 (11)	
Hypertension, *n* (%)	82 (77)	25 (86)	18 (82)	11 (65)	28 (74)	0.3349
Diabetes mellitus, *n* (%)	41 (39)	8 (28)	12 (55)	6 (35)	15 (39)	0.2689
Smoking, *n* (%)	44 (42)	9 (31)	11 (50)	10 (59)	14 (37)	0.221
Dyslipidaemia, *n* (%)	61 (58)	15 (52)	14 (64)	11 (65)	21 (55)	0.7592
Family history, *n* (%)	24 (23)	7 (24)	5 (23)	3 (18)	9 (24)	0.9595
AF history, *n* (%)	51 (48)	13 (45)	11 (50)	7 (41)	20 (53)	0.8332
AF during echo, *n* (%)	49 (41)	7 (24)	10 (40)	3 (18)	24 (62)	0.003
Previous cardiac surgery, *n* (%)	23 (22)	1 (3)	7 (32)	4 (25)	11 (29)	0.0415
COPD, *n* (%)	25 (24)	2 (7)	8 (36)	7 (41)	8 (21)	0.023
CKD stage, *n* (%)						0.6959
1	5 (5)	0 (0)	2 (9)	0 (0)	3 (8)	
2	6 (6)	1 (3)	1 (5)	2 (12)	2 (5)	
3	18 (17)	4 (14)	4 (18)	3 (18)	7 (18)	
4	5 (5)	2 (7)	0 (0)	0 (0)	3 (8)	
Known heart disease, *n* (%)						0.0992
Ischaemic	44 (42)	7 (24)	11 (50)	12 (71)	14 (37)	
Valvular	19 (18)	6 (21)	7 (32)	0 (0)	6 (16)	
Idiopathic	18 (17)	6 (21)	1 (5)	4 (24)	7 (18)	
Tachycardiomyopathy	6 (6)	2 (7)	1 (5)	0 (0)	3 (8)	
Infiltrative	3 (3)	0 (0)	1 (5)	0 (0)	2 (5)	
Hypertrophic	1 (1)	0 (0)	0 (0)	0 (0)	1 (3)	
Other/NA	15 (14)	8 (28)	1 (5)	1 (6)	5 (13)	
Therapy, *n* (%)						
Beta-blockers	78 (75)	19 (66)	17 (85)	11 (65)	31 (82)	0.2313
ACEis/ARBs	53 (51)	17 (59)	9 (45)	8 (47)	19 (50)	0.7812
CCBs	21 (20)	10 (34)	6 (30)	1 (6)	4 (11)	0.0264
MRAs	47 (45)	12 (41)	13 (65)	7 (41)	15 (39)	0.2688
ARNIs	6 (6)	1 (3)	0 (0)	1 (6)	4 (11)	0.3773
PH-specific therapy	2 (2)	1 (3)	1 (5)	0 (0)	0 (0)	0.4689
Echocardiography						
EDDi (cm/m^2)	3.0 ± 0.6	2.9 ± 0.6	3.0 ± 0.7	3.2 ± 0.5	3.1 ± 0.6	0.2171
EDVi (mL/m^2)	73 ± 34	64 ± 27	64 ± 29	87 ± 30	79 ± 37	0.0374
ESVi (mL/m^2)	46 ± 31	35 ± 23	38 ± 26	61 ± 28	54 ± 33	0.0045
EF (%)	41.4 ± 15.8	49.4 ± 14.6	45.9 ± 16.5	33.1 ± 12.9	35.0 ± 13.8	<0.0001
SV (mL)	45 ± 15	49 ± 17	47 ± 15	47 ± 13	40 ± 13	0.0780
CO (L/min)	3.51 ± 1.07	3.61 ± 1.31	3.73 ± 1.08	3.59 ± 1.29	3.27 ± 0.8	0.4723
CI ($L/min/m^2$)	1.94 ± 0.64	2.03 ± 0.75	2.00 ± 0.68	1.98 ± 0.66	1.77 ± 0.55	0.426
LA area (cm^2)	26.6 ± 7.9	23.9 ± 6.8	28.1 ± 7.0	25.8 ± 6.3	28.1 ± 9.3	0.1471
LAVi (mL/m^2)	51 ± 24	46 ± 19	54 ± 22	48 ± 13	54 ± 30	0.4474
RAVi (mL/m^2)	38 ± 23	23 ± 10	34 ± 17	31 ± 14	56 ± 27	<0.0001
RAPLS (%)	20.9 ± 13.0	33.1 ± 13.3	22.5 ± 10.2	20.4 ± 6.9	10.3 ± 4.2	<0.0001
TAPSE (mm)	15.7 ± 4.7	18.3 ± 4.6	17.3 ± 4.5	15.1 ± 3.4	12.7 ± 3.9	<0.0001
FAC (%)	35.7 ± 13.4	39.8 ± 13.1	41.2 ± 12.9	34.8 ± 16.1	29.3 ± 11.9	0.0166
RV TDI S′ velocity (cm/s)	9.4 ± 3.1	11.3 ± 3.6	9.6 ± 2.0	9.1 ± 2.9	7.7 ± 2.3	0.0002
E/E′	16.21 ± 8.29	12.68 ± 6.47	21.32 ± 11.29	15.47 ± 4.94	16.71 ± 7.75	0.0060
TR severity, *n* (%)						<0.0001
Mild	57 (48)	22 (76)	16 (64)	9 (53)	4 (10)	
Moderate	36 (30)	5 (17)	8 (32)	5 (29)	16 (41)	
Severe	16 (13)	2 (7)	0 (0)	3 (18)	10 (26)	
Massive or torrential	10 (8)	0 (0)	1 (4)	0 (0)	9 (23)	
TR velocity (cm/s)	2.87 ± 0.58	2.68 ± 0.5	2.97 ± 0.71	2.81 ± 0.43	3 ± 0.63	0.2511
RV–RA grad (mmHg)	33.1 ± 14.6	28.8 ± 12.5	35.9 ± 18.8	33.7 ± 10.1	35.2 ± 15.8	0.3310
PASP (mmHg)	44.1 ± 17.3	34.0 ± 13.4	44.0 ± 19.9	47.4 ± 9.4	50.6 ± 17.3	0.0004
TAPSE/PASP (mm/mmHg)	0.41 ± 0.22	0.6 ± 0.23	0.44 ± 0.15	0.34 ± 0.14	0.27 ± 0.10	<0.0001
IVC expiratory diameter (cm)	1.93 ± 0.60	1.57 ± 0.42	1.62 ± 0.42	2.11 ± 0.49	2.28 ± 0.63	<0.0001

(*Continues*)

Table 1 (continued)

	All (119)	Continuous (29)	Pulsatile (25)	Biphasic (17)	Monophasic (39)	*P* value
IVC inspiratory diameter (cm)	1.22 ± 0.69	0.71 ± 0.39	0.84 ± 0.39	1.66 ± 0.67	1.71 ± 0.62	<0.0001
CI (%)	41 ± 22	57 ± 17	51 ± 16	27 ± 19	26 ± 16	<0.0001
eRAP (mmHg)	10 ± 4.1	7.2 ± 3.2	7.8 ± 3.5	12.5 ± 3.4	12.5 ± 3.3	<0.0001
Renal Doppler						
RRI	0.68 ± 0.11	0.68 ± 0.09	0.66 ± 0.09	0.7 ± 0.08	0.68 ± 0.14	0.7681
VII		0.15 (0.08–0.32)				
RVSI	0.56 (0.35–0.75)		0.22 (0.15–0.36)	0.54 (0.42–0.60)	0.75 (0.64–0.78)	<0.0001
Laboratory data						
Creatinine (mg/dL)	1.27 ± 0.49	1.22 ± 0.57	1.15 ± 0.43	1.39 ± 0.56	1.34 ± 0.48	0.3568
eGFR (mL/min)	57 ± 20	59 ± 23	60 ± 20	55 ± 23	55 ± 18	0.6923
Na (mEq/L)	140 ± 3	141 ± 2	140 ± 4	140 ± 2	140 ± 4	0.1669
Hb (g/dL)	12.4 ± 2.0	12.8 ± 2.1	12.3 ± 2.4	12.2 ± 1.7	12.4 ± 1.8	0.7525
NT-proBNP (ng/L)	3229 (1498–7287)	2135 (617–3618)	2367 (1512–6381)	6457 (2346–21 839)	4044 (2405–9073)	<0.0001

ACEis, angiotensin-converting enzyme inhibitors; AF, atrial fibrillation; ARBs, angiotensin receptor blockers; ARNIs, angiotensin receptor neprilysin inhibitors; BSA, body surface area; CCBs, calcium channel blockers; CI, cardiac index; CKD, chronic kidney disease; CO, cardiac output; COPD, chronic obstructive pulmonary disease; EDDi, end-diastolic diameter index; EDVi, end-diastolic volume index; EF, ejection fraction; eGFR, estimated glomerular filtration rate; eRAP, estimated right atrial pressure; ESVi, end-systolic volume index; FAC, fractional area change; IVC, inferior vena cava; LA, left atrial; LAVi, left atrial volume index; MRAs, mineralocorticoid receptor antagonists; NT-proBNP, N-terminal pro-brain natriuretic peptide; NYHA, New York Heart Association; PASP, pulmonary artery systolic pressure; PH, pulmonary hypertension; RA, right atrial; RAPLS, right atrial peak longitudinal strain; RAVi, right atrial volume index; RRI, renal resistive index; RV, right ventricular; RVSI, renal venous stasis index; SV, stroke volume; TAPSE, tricuspid annular plane systolic excursion; TDI, tissue Doppler imaging; TR, tricuspid regurgitation.

No differences of IRVF pattern were observed according to age, sex, NYHA class, aetiology of HF, cardiovascular risk factors prevalence, and baseline renal function (evaluated by CKD stage, serum creatinine, and eGFR). As for the latter, because no paired data on renal function–IRVF pattern at follow-up are available, the relation cannot be adequately evaluated.

Patients with COPD or previous cardiac surgery showed a significantly higher discontinuous IRVF patterns. As anticipated, COPD patients had significantly higher PASP and lower TAPSE/PASP ratio values. Instead, post-surgery subjects exhibited a lower TAPSE, S'-wave velocity, and RAPLS, with non-significant differences in TAPSE/PASP ratio (P = 0.058), PASP (P = 0.902), and FAC (P = 0.374).

No differences were observed in home therapeutic regimens, except for calcium channel blocker (CCB) intake, which was linked to a better renal venous flow pattern. As expected, patients receiving CCB medications had significantly higher EF compared with others (49 ± 16% vs. 39 ± 15%, P = 0.006).

AF history did not differ across the IRVF spectrum, whereas, during IRVF recording, AF was more prevalent in the monophasic group (P = 0.003). Normal continuous IRVF pattern exhibited smaller LV volume and higher EF, although no differences in SV, CO, and CI were noted. Left atrial volume index (LAVi) did not differ between IRVF groups, while higher RAVi and lower strain values (RAPLS) were associated with discontinuous renal flow patterns.

RV dimensions were smaller, and function parameters were better (TAPSE, S'-wave velocity, and FAC) in patients with continuous vs. discontinuous IRVF pattern.

Interestingly, a lower TAPSE/PASP ratio and a higher PASP coupled with discontinuous patterns. Similarly, higher IVC diameter, lower IVC collapsibility ratio, higher eRAP, and more severe degrees of TR were more common in the discontinuous group. RVSI progressively increased from pulsatile to monophasic group, reflecting worsening degrees of renal congestion, whereas no differences in RRI were observed. NT-proBNP levels were higher in patients with discontinuous IRVF patterns. RVSI correlation analysis is reported in Supporting Information, *Results* and *Table S1*.

TAPSE/PASP ratio distribution is reported in Supporting Information, *Results* and *Table S2*.

Univariate and multivariate regression analyses

Univariate regression analysis of RVSI was performed, and RV function parameters like TAPSE, S'-wave velocity, FAC, and TAPSE/PASP ratio resulted as significantly associated factors. The same was true for RA parameters (RAPLS and RAVi), IVC diameters and eRAP, severity of TR, PASP, and LV EF. No significant association was found regarding LV dimensions and volumes, haemodynamic indexes, and baseline renal function (*Table 2*).

To further explore the independent determinants of RVSI, a multivariate linear regression analysis model of significant univariate factors was performed. Interestingly, TAPSE/PASP ratio, RAPLS, and IVC expiratory diameter emerged as significant independent RVSI determinants (R^2 = 0.617) (*Table 3*).

Interestingly, the degree of TR (severe vs. non-severe) did not result as an independent RVSI determinant. Similar

Table 2 RVSI univariate linear regression analysis

	β (SE)	t	P value
TAPSE/PASP	−1.08 (0.13)	−8.08	<0.0001
EF	−0.00 (0.00)	−3.29	0.0015
SVi	0.00 (0.00)	−1.95	0.0550
CO	0.03(0.03)	−0.92	0.3632
LAVi	0.00 (0.00)	0.88	0.3795
TAPSE	0.03 (0.00)	−5.99	<0.0001
FAC	−0.01 (0.00)	−4.44	<0.0001
RV TDI S′ velocity	−0.05 (0.01)	−3.96	0.0002
TR velocity	0.04 (0.05)	0.75	0.4558
TR severity	0.17 (0.03)	6.43	<0.0001
E/E′	−0.00(0.00)	−0.59	0.5571
PASP	0.00 (0.00)	2.13	0.0361
IVC expiratory diameter	0.16 (0.04)	4.23	<0.0001
CI	−0.00 (0.00)	−4.94	<0.0001
Creatinine	0.08 (0.05)	1.60	0.1134
eGFR	−0.00 (0.00)	−1.00	0.3217
NT-proBNP	0.00 (0.00)	1.45	0.1501
Na^+	−0.00(0.00)	−1.54	0.8413
RRI	0.16 (0.24)	0.67	0.5030
RAPLS	−0.02 (0.00)	−6.86	<0.0001

CI, cardiac index; CO, cardiac output; EF, ejection fraction; eGFR, estimated glomerular filtration rate; FAC, fractional area change; IVC, inferior vena cava; LAVi, left atrial volume index; NT-proBNP, N-terminal pro-brain natriuretic peptide; PASP, pulmonary artery systolic pressure; RAPLS, right atrial peak longitudinal strain; RRI, renal resistive index; RV, right ventricular; RVSI, renal venous stasis index; SVi, stroke volume index; TAPSE, tricuspid annular plane systolic excursion; TDI, tissue Doppler imaging; TR, tricuspid regurgitation.

Table 3 Multivariate linear regression analysis of RVSI determinants

R^2		Root MSE	RVSI mean	
0.617116		0.195542	0.403763	
Parameter	Estimate	SE	t value	$Pr > \|t\|$
Intercept	0.592008	0.108250	5.468917	<0.0001
TAPSE/PASP	−0.606472	0.139613	−4.343959	<0.0001
IVC expiratory diameter	0.106349	0.038810	2.740233	0.007
RAPLS	−0.007644	0.002231	−3.426625	<0.0001

IVC, inferior vena cava; MSE, mean standard error; PASP, pulmonary artery systolic pressure; RAPLS, right atrial peak longitudinal strain; RVSI, renal venous stasis index; TAPSE, tricuspid annular plane systolic excursion.

results were obtained when stratifying patients by NT-proBNP tertiles and with IVC expiratory diameter ≥21 mm. However, in patients with non-dilated IVC (i.e. <21 mm), more than moderate TR resulted as a significant predictor of renal congestion (P = 0.026) (*Table 4*).

Composite endpoint

Kaplan–Meier cumulative survival curves are presented for TAPSE/PASP, RVSI, and NT-proBNP tertiles and compared using the log-rank test (*Figure 3*). At multivariate analysis, variables significantly associated with the primary composite endpoint were RVSI and NT-proBNP (*Table 5*). Of note, renal Doppler was the only echo-derived haemodynamic parameter with prognostic significance.

Outcome analysis and follow-up

Thirty-three patients (27%) were lost at follow-up. During the observation period (median 24 months, IQR 17–39 months; range 1–47 months), 43 patients (50%) met the primary endpoint. Twenty-six patients died from cardiovascular disease (20 pump failure and 6 arrhythmic event), 14 patients experienced at least one unplanned hospitalization from HF, and 3 patients underwent haemodialysis due to severe renal function worsening.

Receiver operating characteristic curve analysis and score derivation

Based on the multivariate analysis, we modelled a score to predict severe renal congestion by combining RAPLS, TAPSE/PASP ratio, IVC expiratory diameter, and degree of TR as main determinants of renal congestion. One point was attributed for a marked abnormality of the following parameters: TAPSE/PASP ratio ≤0.30, RAPLS ≤ 20%, IVC expiratory diameter ≥21 mm, and more than mild TR (*Figure 4*). A RAPLS ≤ 20% was taken as an indicator of RA dysfunction based on reported normal values.[19] The TAPSE/PASP ratio cut-off of 0.30 was selected on published data[12] and corresponded also to the lower tertile of our sample. An IVC expiratory diameter ≥21 mm is the pathological cut-off by the current guidelines.[10] Furthermore, inclusion of TR was based on previous reports.[4,6,20] To test the score diagnostic performance (i.e. identification of severe vs. non-severe renal congestion), results were compared with the actual renal Doppler data and ROC curves were calculated. A score of 3 provided the best diagnostic accuracy for monophasic IRVF pattern [sensitivity of 80%, specificity of 87%, diagnostic accuracy of 84%, area under the ROC curve (AUC) of 0.898, $P < 0.0001$] or an RVSI ≥ 0.75 (sensitivity of 91%, specificity of 89%, diagnostic accuracy of 89%, AUC of 0.904, $P < 0.0001$; *Figure 5*) identification. The intra-observer and inter-observer reproducibility is reported in the Supporting Information.

Discussion

The evaluation of intra-renal haemodynamics by means of echo-Doppler imaging is steadily emerging and receiving progressive attention as a relevant clinical tool in the diagnostic armamentarium and clinical management of

Table 4 Multivariate linear regression analysis of RVSI determinants when IVC < 21 mm

R^2		Root MSE	RVSI mean	
0.560173		0.196343	0.278000	
Parameter	Estimate	SE	*t* value	$Pr > \|t\|$
Intercept	0.681168	0.067175	10.140132	<0.0001
TAPSE/PASP	−0.639034	0.158625	−4.028574	<0.0001
TR > moderate	0.206991	0.088407	2.341345	0.228
RAPLS	−0.005212	0.002406	−2.165905	0.0346

IVC, inferior vena cava; MSE, mean standard error; PASP, pulmonary artery systolic pressure; RAPLS, right atrial peak longitudinal strain; RVSI, renal venous stasis index; TAPSE, tricuspid annular plane systolic excursion; TR, tricuspid regurgitation.

Figure 3 Kaplan–Meier curves of (A) renal venous stasis index, (B) tricuspid annular plane systolic excursion/pulmonary artery systolic pressure, and (C) N-terminal pro-brain natriuretic peptide.

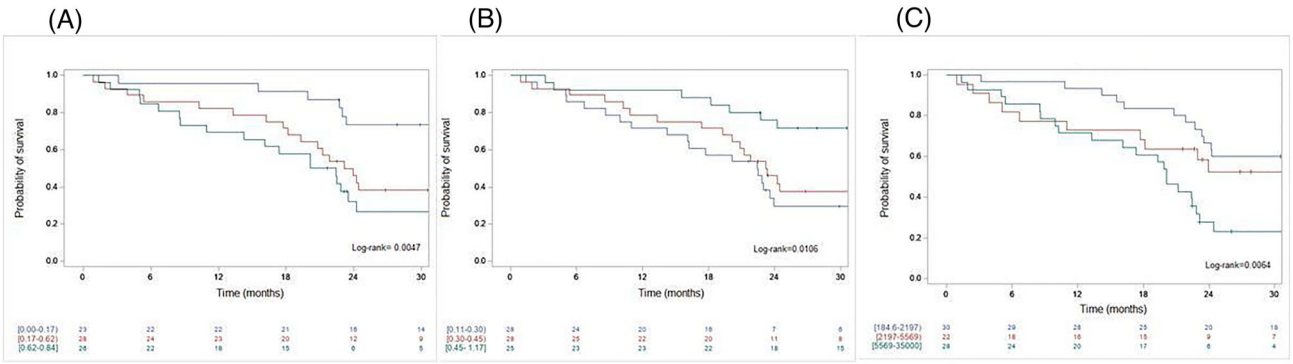

Table 5 Univariate and multivariate analyses of variables associated with primary endpoint

	Univariate			Multivariable		
	HR	95% CI	*P* value	HR	95% CI	*P* value
TAPSE/PASP	0.085	0.014–0.525	0.0080	1.944	0.118–32.026	0.6419
RVSI	8.359	2.656–26.308	0.0003	6.614	0.984–44.474	0.0520
RAPLS	0.974	0.947–1.002	0.0640	—	—	—
IVC expiratory diameter	1.441	0.877–2.369	0.1498	—	—	—
TR severity	1.294	0.953–1.759	0.0990	—	—	—
NT-proBNP	1.005	1.002–1.008	0.0006	1.009	1.004–1.013	0.0002
Creatinine	1.786	1.062–3.003	0.0286	1.623	0.846–3.113	0.1455
EDVi	1.006	0.997–1.014	0.1979	—	—	—
EF	0.985	0.965–1.006	0.0135	1.019	0.987–1.051	0.2454
CO	0.876	0.615–1.248	0.4633	—	—	—
E/e'	0.995	0.958–0.995	0.7742	—	—	—

CI, confidence interval; CO, cardiac output; EDVi, end-diastolic volume index; EF, ejection fraction; HR, hazard ratio; IVC, inferior vena cava; NT-proBNP, N-terminal pro-brain natriuretic peptide; PASP, pulmonary artery systolic pressure; RAPLS, right atrial peak longitudinal strain; RVSI, renal venous stasis index; TAPSE, tricuspid annular plane systolic excursion; TR, tricuspid regurgitation.

congestion in HF.[20,21] Our data point on a combined source of information through the definition of the renal Doppler 'congestive phenotype' and the right heart dynamics reporting the first analysis of renal blood flow characteristics in AHF. Notably, RVSI emerged as the only haemodynamic variable predictive of clinical events. We also report a pragmatic echocardiographic score correlating with renal congestion at presentation.

Implications of renal flow analysis in acute heart failure

Renal function deterioration in HF is the result of the complex interaction and balance of various extravascular and intravascular determinants that yield a reduced net glomerular capillary blood flow and filtration pressure. Those factors include, for example, renal hypoperfusion beyond

Figure 4 Four-elements echo score to predict renal congestion. One point is assigned to tricuspid annular plane systolic excursion (TAPSE)/pulmonary artery systolic pressure (PASP) ratio ≤0.30, right atrial peak longitudinal strain (RAPLS) ≤20%, inferior vena cava (IVC) expiratory diameter ≥21 mm, or more than mild tricuspid regurgitation. Marked renal congestion (i.e. monophasic intra-renal venous flow pattern or renal venous stasis index ≥0.75) is likely reflected by a score ≥3.

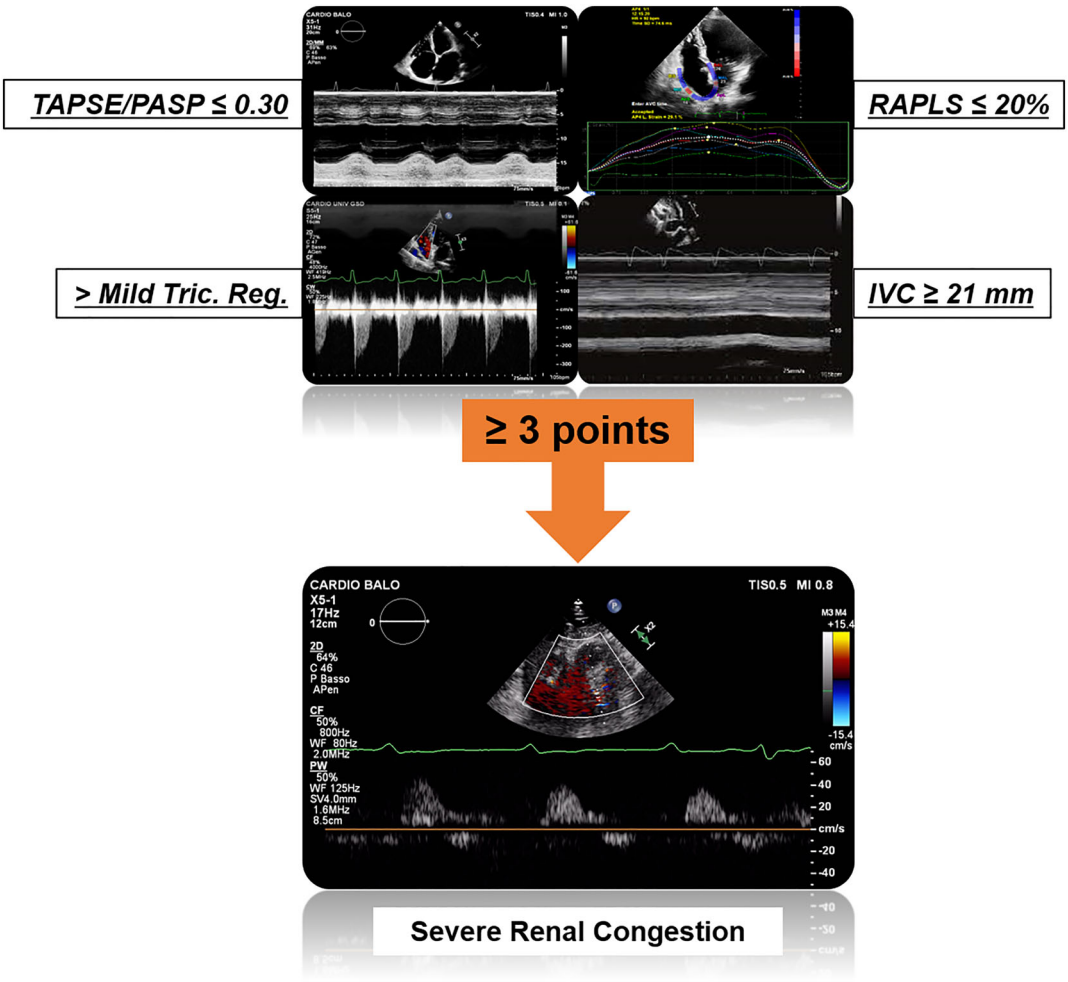

autoregulatory range (perfusion pressure ≤80 mmHg), HF-induced up-regulation of sympathetic nervous and renin–angiotensin–aldosterone (RAS) systems, intra-abdominal hypertension, increased interstitial renal pressure, and dysregulation of gut flora and endothelial function.[22] Initial triggers of these abnormalities are a RAP elevation and renal stasis, promoting splanchnic and gut venous congestion as classically described by Guyton's model.[23,24] The identification of renal congestion by IRVF pattern is simple and feasible in most patients and carries important prognostic implications. Previous works have shown that mortality and renal function deterioration markedly increase in HF patients with renal congestion during hospital admission or at follow-up,[4–6] especially when RV dysfunction is present.[9] It was also demonstrated that IRVF may change acutely according to volume status and decongestive therapies.[8,17] In this scenario, data on AHF patients are lacking and thorough determinants of the renal congestion besides RAP elevation are still elusive.

The haemodynamic profile of our patients closely matches the one of previous data, with the only exception of a lower EF among the discontinuous IRVF patterns, which is likely explained by the higher prevalence of reduced EF patients in our AHF sample, compared with the relatively preserved and homogenous EF reported in previous works involving stable/chronic HF patients.[2,4,20] When compared with the other single work published on AHF patients,[9] our population showed slightly worse RV function (mean TAPSE 16 vs. 18 mm) and CO (3.5 vs. 4.7 L/min), while PASP was marginally lower (44 vs. 54 mmHg). Other significant haemodynamic, renal Doppler, laboratory, and demographic parameters were almost identical (EF, eRAP, discontinuous IRVF pattern prevalence, serum creatinine, eGFR, NT-proBNP, age, and NYHA class).

Figure 5 Receiver operating characteristic curves of echo renal congestion score performance. A score of 3 identified in patients with a monophasic intra-renal venous flow (IRVF) pattern (top) shows a sensitivity and specificity of 80% and 87%, respectively, with a diagnostic accuracy of 84% [area under the ROC curve (AUC) of 0.898, $P < 0.0001$]. Similarly, a score of 3 was associated with renal venous stasis index (RVSI) ≥0.75 (bottom) (sensitivity of 91%, specificity of 89%, diagnostic accuracy of 89%, AUC of 0.904, $P < 0.0001$).

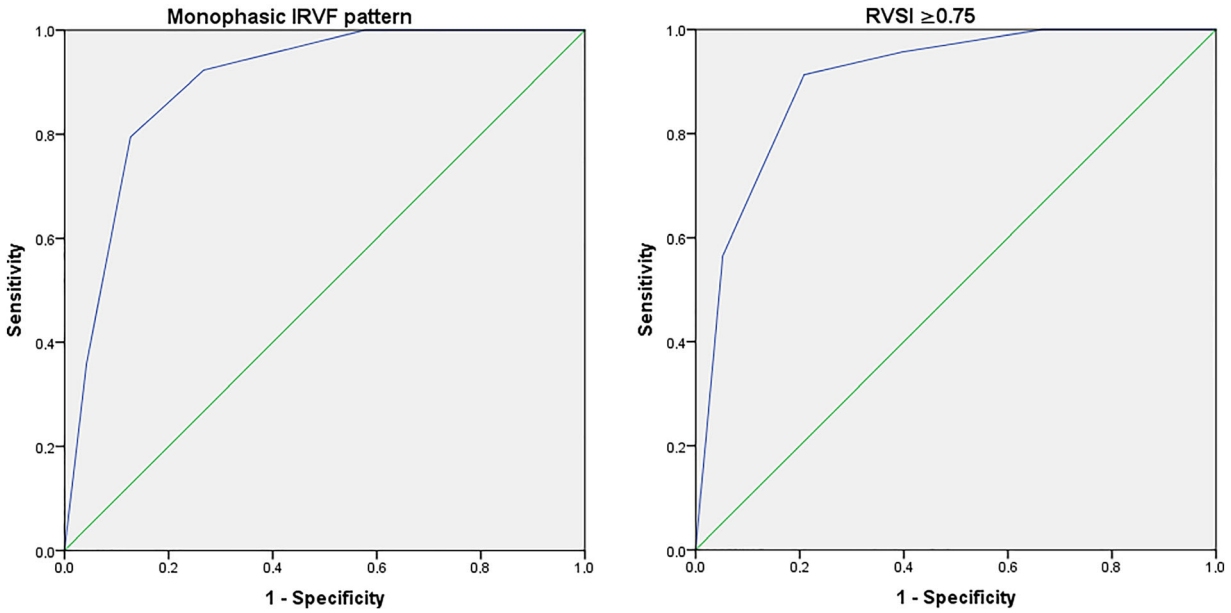

Also, previous works[4,6] report a slight decline in renal function over the IRVF congestive spectrum. No differences were observed in our populations, as it may be expected in AHF.[6]

Because renal congestion evaluated by RVSI proved to be a highly prognostic parameter in this population of HF patients, we suggest incorporating its routine measurement in clinical practice.

Interaction between renal flow, right atrial dynamics, and right ventricular to pulmonary circulation coupling

The relation between RAP and venous return, a matter debated for decades by physiologists, is not univocal with both variables each other dependent on a dynamic equilibrium of pulmonary engorgement, cardiac, and systemic venous return function.[9] Besides the single numerical value of RAP, conventionally measured at the end-expiratory pre-C point, a role also for pressure waveform morphology as contributor to determine the effective renal venous outflow has been anticipated. Our findings extend on the role of an elevated RAP together with impaired right atrioventricular dynamics as mechanical mediators of the backward pulsatile load impeding the normal venous outflow, configuring the pathophysiological hallmark of renal stasis. Specifically, the combined contribution of both atrial and ventricular functions, along with the presence and degree of tricuspid valve pathology, is key elements.[20] Remarkably, identical RAPs may match with different combinations of the aforementioned factors yielding to specific degrees of renal venous congestion and venous flow disruption, as shown in *Figure 6*.

For example, advanced RV dysfunction or TR combines with marked elevation of the jugular pulse x-descent and v-wave; similarly, when the compensatory increase in RA function to maintain RV filling (the so-called preload reserve) is exhausted, a-wave elevation ensues, possibly leading to abnormal renal venous flow despite normal RAP values.[20,25]

Statistical analysis of univariate and multivariate determinants of RVSI highlighted TAPSE/PASP ratio, RAPLS, and IVC expiratory diameter as significant and independent parameters, thus suggesting a crucial role of the right heart in determining renal congestion in AHF, regardless of left heart function. This finding, although previously anticipated, has never been the subject of a dedicated investigation to validate it.

In addition, while a role for TR in determining splanchnic stasis may be expected and has been extensively described, in our AHF population, it became independently relevant only among patients with a near-normal intravascular volume (i.e. IVC < 21 mm).

Although we do not have a definite explanation, we think these findings may be explained by the dynamic nature and exquisite volume dependency of TR.

In patients with marked fluid overload, a certain degree of functional TR is expected, which may not be independently responsible for venous stasis but rather act as 'proportionate' TR. However, when the severity of regurgitation exceeds the

Figure 6 (A) Positive pressure gradient (grey) between the mean systemic filling pressure (dotted line) and systemic veins, in the presence of normal right atrial pressure (RAP) and regular jugular venous pulse morphology [no significant right ventricular (RV) or right atrial (RA) dysfunction or tricuspid valve disease]. (B) Pressure gradient is reduced (grey) when RAP is elevated, leading to discontinuous venous outflow. (C) Marked reduction in venous flow (grey) due to jugular waveform disruption (as with RV or RA pathology or tricuspid valve disease), independently from RAP values.

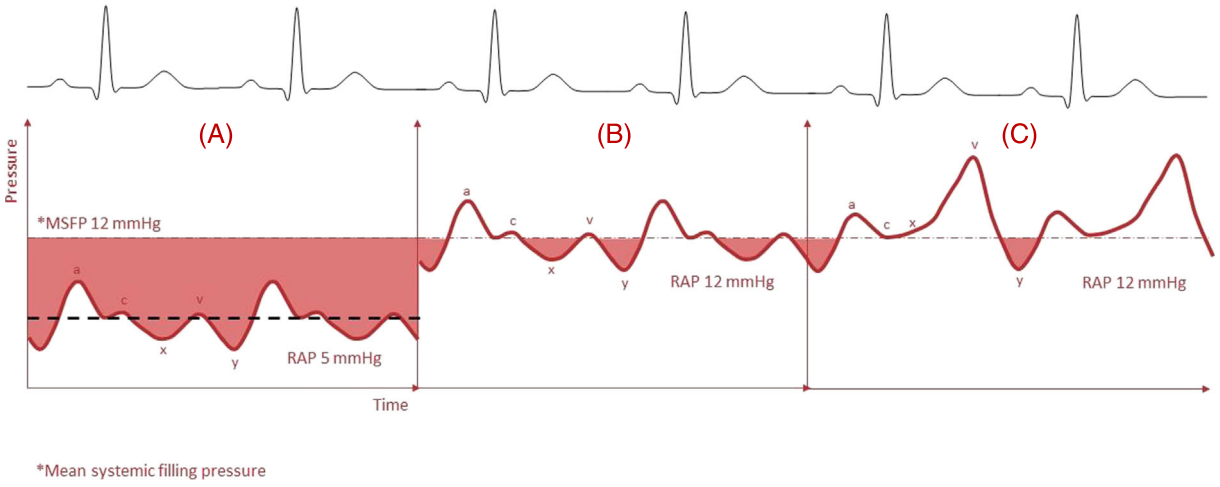

degree of intravascular congestion, it may disrupt splanchnic venous outflow. Again, to fully support this hypothesis, a longitudinal follow-up during decongestion would be needed.

Renal phenotyping score

We here propose a simple echocardiographic score integrating relevant parameters to identify severe degrees of renal congestion as a surrogate for renal Doppler evaluation, which, albeit simple and reproducible, may not yet be routinely endorsed by cardiologists in clinical practice. We anticipate that a simple tool like a score may encourage and simplify patient assessment and help to identify those with an advanced congestive phenotype, warranting more aggressive volume depleting therapy. However, because paired data on score values and renal Doppler profile were collected only at admission, the findings cannot be extended to predict renal congestion at discharge and follow-up.

Study limitations

This is a relatively small sample size study requiring observational longitudinal studies. Moreover, due to its single-centre and single-unit design, patient selection may suffer of some biases, especially excluding AHF patients acutely admitted to intensive care unit (ICU). No invasive data of atrial, pulmonary, and RV pressures were available. The lack of an RV strain analysis with its ratio derivation with PASP may generate some lack in precision. Nonetheless, the TAPSE/PASP analysis is the only non-invasive echo-derived method validated against RV pressure volume curves. As to the proposed echocardiographic score, a validation process across centres is required. Moreover, a serial reassessment during decongestive therapy is warranted, and most importantly, it should be correlated with changes in renal pattern to verify whether it can actually describe and predict its fluctuations.

Conclusions

Phenotyping renal congestion in AHF through renal Doppler analysis combined with a right heart haemodynamics appears feasible and informative. The integration of ultrasound-derived right heart and kidney flow variables into a four-element echocardiographic score seems a simple and effective tool to identify the renal congestive phenotype of AHF when renal flow analysis is not available. Present findings extend the evidence on the cardio-renal syndrome approach, paving the way to intervention strategies with proven effectiveness on the right heart that may benefit the kidney.

Conflict of interest

None declared.

Funding

The present investigation was supported by a grant of the Fondazione Italo Monzino, Milan, Italy.

Supporting information

Additional supporting information may be found online in the Supporting Information section at the end of the article.

Table S1. RVSI Correlation Analysis.
Table S2. Demographic, Clinical Characteristics, Echocardiographic, and Laboratory Data according to TAPSE/PASP Ratio.

Figure S1. Example of a patient's right atrial strain curve at admission: RAPLS 14%. The patient had a monophasic venous flow pattern and a TAPSE/PASP ratio of 0.22, A. The same patient after decongestion was achieved: RAPLS improved to 28.9%, IRVF pattern became continuous and TAPSE/PASP ratio increased to 0.49, B (*readapted to match scale with A*). ε_s: reservoir function. ε_e conduit function. ε_a: booster function.

References

1. Damman K, Valente MA, Voors AA, O'Connor CM, van Veldhuisen DJ, Hillege HL. Renal impairment, worsening renal function, and outcome in patients with heart failure: An updated meta-analysis. *Eur Heart J* 2014;**35**:455–469. doi:10.1093/eurheartj/eht386
2. Husain-Syed F, Grone HJ, Assmus B, Bauer P, Gall H, Seeger W, *et al*. Congestive nephropathy: A neglected entity? Proposal for diagnostic criteria and future perspectives. *ESC Heart Fail* 2021;**8**:183–203. doi:10.1002/ehf2.13118
3. Jeong SH, Jung DC, Kim SH. Renal venous Doppler ultrasonography in normal subjects and patients with diabetic nephropathy: Value of venous impedance index measurements. *J Clin Ultrasound* 2011;**39**:512–518. doi:10.1002/jcu.20835
4. Iida N, Seo Y, Sai S, Machino-Ohtsuka T, Yamamoto M, Ishizu T, *et al*. Clinical implications of intrarenal hemodynamic evaluation by Doppler ultrasonography in heart failure. *JACC Heart Fail* 2016;**4**:674–682. doi:10.1016/j.jchf.2016.03.016
5. Yamamoto M, Seo Y, Iida N, Ishizu T, Yamada Y, Nakatsukasa T, *et al*. Prognostic impact of changes in intrarenal venous flow pattern in patients with heart failure. *J Card Fail* 2021;**27**:20–28. doi:10.1016/j.cardfail.2020.06.016
6. Husain-Syed F, Birk HW, Ronco C, Schörmann T, Tello K, Richter MJ, *et al*. Doppler-derived renal venous stasis index in the prognosis of right heart failure. *J Am Heart Assoc* 2019;**8**:e013584. doi:10.1161/JAHA.119.013584
7. Beaubien-Souligny W, Benkreira A, Robillard P, Bouabdallaoui N, Chassé M, Desjardins G, *et al*. Alterations in portal vein flow and intrarenal venous flow are associated with acute kidney injury after cardiac surgery: A prospective observational cohort study. *J Am Heart Assoc* 2018;**7**:e009961. doi:10.1161/JAHA.118.009961
8. Ter Maaten JM, Dauw J, Martens P, Somers F, Damman K, Metalidis C, *et al*. The effect of decongestion on intrarenal venous flow patterns in patients with acute heart failure. *J Card Fail* 2021;**27**:29–34. doi:10.1016/j.cardfail.2020.09.003
9. Bouabdallaoui N, Beaubien-Souligny W, Denault AY, Rouleau JL. Impacts of right ventricular function and venous congestion on renal response during depletion in acute heart failure. *ESC Heart Fail* 2020;**7**:1723–1734. doi:10.1002/ehf2.12732
10. McDonagh TA, Metra M, Adamo M, Gardner RS, Baumbach A, Böhm M, *et al*. Corrigendum to: 2021 ESC guidelines for the diagnosis and treatment of acute and chronic heart failure: Developed by the Task Force for the Diagnosis and Treatment of Acute and Chronic Heart Failure of the European Society of Cardiology (ESC) with the special contribution of the Heart Failure Association (HFA) of the ESC. *Eur Heart J* 2021. doi:10.1093/eurheartj/ehab670
11. Lang RM, Badano LP, Mor-Avi V, Afilalo J, Armstrong A, Ernande L, *et al*. Recommendations for cardiac chamber quantification by echocardiography in adults: An update from the American Society of Echocardiography and the European Association of Cardiovascular Imaging. *J Am Soc Echocardiogr* 2015;**28**:e14. doi:10.1016/j.echo.2014.10.003
12. Guazzi M, Bandera F, Pelissero G, Castelvecchio S, Menicanti L, Ghio S, *et al*. Tricuspid annular plane systolic excursion and pulmonary arterial systolic pressure relationship in heart failure: An index of right ventricular contractile function and prognosis. *Am J Physiol Heart Circ Physiol* 2013;**305**:H1373–H1381. doi:10.1152/ajpheart.00157.2013
13. Tello K, Wan J, Dalmer A, Vanderpool R, Ghofrani HA, Naeije R, *et al*. Validation of the tricuspid annular plane systolic excursion/systolic pulmonary artery pressure ratio for the assessment of right ventricular-arterial coupling in severe pulmonary hypertension. *Circ Cardiovasc Imaging* 2019;**12**:e009047. doi:10.1161/CIRCIMAGING.119.010059
14. Badano LP, Kolias TJ, Muraru D, Abraham TP, Aurigemma G, Edvardsen T, *et al*. Standardization of left atrial, right ventricular, and right atrial deformation imaging using two-dimensional speckle tracking echocardiography: A consensus document of the EACVI/ASE/Industry Task Force to standardize deformation imaging. *Eur Heart J Cardiovasc Imaging* 2018;**19**:591–600. doi:10.1093/ehjci/jey042
15. Jain S, Kuriakose D, Edelstein I, Ansari B, Oldland G, Gaddam S, *et al*. Right atrial phasic function in heart failure with preserved and reduced ejection fraction. *JACC Cardiovasc Imaging* 2019;**12**:1460–1470. doi:10.1016/j.jcmg.2018.08.020
16. Hahn RT, Zamorano JL. The need for a new tricuspid regurgitation grading scheme. *Eur Heart J Cardiovasc Imaging* 2017;**18**:1342–1343. doi:10.1093/ehjci/jex139
17. Nijst P, Martens P, Dupont M, Tang WHW, Mullens W. Intrarenal flow alterations during transition from euvolemia to intravascular volume expansion in heart failure patients. *JACC Heart Fail* 2017;**5**:672–681. doi:10.1016/j.jchf.2017.05.006
18. Viazzi F, Leoncini G, Derchi LE, Pontremoli R. Ultrasound Doppler renal resistive index: A useful tool for the management of the hypertensive patient. *J Hypertens* 2014;**32**:149–153. doi:10.1097/HJH.0b013e328365b29c
19. Peluso D, Badano LP, Muraru D, Dal Bianco L, Cucchini U, Kocabay G, *et al*. Right atrial size and function assessed with three-dimensional and speckle-tracking echocardiography in 200 healthy volunteers. *Eur Heart J Cardiovasc Imaging* 2013;**14**:1106–1114. doi:10.1093/ehjci/jet024
20. Seo Y, Iida N, Yamamoto M, Ishizu T, Ieda M, Ohte N. Doppler-derived intrarenal venous flow mirrors right-sided heart hemodynamics in patients with cardiovascular disease. *Circ J* 2020;**84**:1552–1559. doi:10.1253/circj.CJ-20-0332
21. Kitai T, Tang WHW. Intrarenal venous flow: A distinct cardiorenal phenotype or simply a marker of venous congestion? *J Card Fail* 2021;**27**:35–39. doi:10.1016/j.cardfail.2020.12.001

22. Afsar B, Ortiz A, Covic A, Solak Y, Goldsmith D, Kanbay M. Focus on renal congestion in heart failure. *Clin Kidney J* 2016;**9**:39–47. doi:10.1093/ckj/sfv124
23. Guyton AC, Lindsey AW, Abernathy B, Richardson T. Venous return at various right atrial pressures and the normal venous return curve. *Am J Physiol* 1957;**189**:609–615.
24. Guazzi M, Gatto P, Giusti G, Pizzamiglio F, Previtali I, Vignati C, *et al*. Pathophysiology of cardiorenal syndrome in decompensated heart failure: Role of lung–right heart–kidney interaction. *Int J Cardiol* 2013; **169**:379–384. doi:10.1016/j.ijcard.2013.09.014
25. Sakata K, Uesugi Y, Isaka A, Minamishima T, Matsushita K, Satoh T, *et al*. Evaluation of right atrial function using right atrial speckle tracking analysis in patients with pulmonary artery hypertension. *J Echocardiogr* 2016;**14**:30–38. doi:10.1007/s12574-015-0270-4